Available online at www.sciencedirect.com

SciVerse ScienceDirect

Ceramics International 39 (2013) 2267–2274

CERAMICS INTERNATIONAL

www.elsevier.com/locate/ceramint

Preparation of high solid loading, low viscosity ZrB_2–SiC aqueous suspensions using PEI as dispersant

Rujie He*, Ping Hu, Xinghong Zhang, Wenbo Han, Chuncheng Wei, Yang Hou

National Key Laboratory of Science and Technology on Advanced Composites in Special Environments, Harbin Institute of Technology, Harbin 150001, PR China

Received 21 May 2012; received in revised form 15 August 2012; accepted 24 August 2012
Available online 1 September 2012

Abstract

PEI was used as dispersant for ZrB_2 and SiC powders in water. The dispersion behavior of ZrB_2 and SiC in water was studied by zeta potential measurements, particle size distribution measurements and interparticle interaction calculations. Well-dispersed ZrB_2 and SiC aqueous suspensions were obtained using 0.6 wt% PEI at pH 6. The rheological behavior of ZrB_2–SiC aqueous suspensions was also investigated. Finally, a high solid loading (52 vol%), low viscosity (980 mPa s at 100 s^{-1}) ZrB_2–SiC aqueous suspension was successfully prepared.

Keywords: A. Suspensions; B. Composites; C. Chemical properties; D. Borides

1. Introduction

ZrB_2–SiC ultra high temperature ceramic (UHTC) composites are thought to be attractive candidates for ultra high temperature structural materials due to their excellent strength under high temperatures [1,2], superb non-ablative properties and good oxidation resistance [3–5]. These properties allow them to be used in extreme environments, including hypersonic flight, atmospheric re-entry and rocket propulsion and so on [6–8].

ZrB_2–SiC composites are usually fabricated by hot-pressing (HP) techniques [9]. However, HP processes always limit the formation of relative simple geometrical and moderate sizes. Fabrication of UHTC components with complex shapes requires costly and time-consuming machining. Increasing attention is, therefore, directed towards colloidal processing methods, which may result in a complex-shaped as well as homogenous microstructure green body. Recently, slip casting [10,11], tape casting [12–15] and some other colloidal techniques [16] have been successfully applied to the preparation of ZrB_2–SiC composites. In our previous research, a novel near-net shape colloidal process, aqueous gelcasting, was successfully applied to prepare ZrB_2–SiC composites [17,18].

In all of these processes, preparing a ceramic suspension with high solid loading and low viscosity is the most key issue. In order to obtain such a ceramic suspension, the chose and control of dispersant, dispersant concentration and pH value must be paid more attention. A ZrB_2–SiC suspension with 50 vol% solid loading was prepared by using polyacrylic acid (PAA, $M_w = 3000$) as dispersant. However, the viscosity was still very high, 3.1 Pa s at the shear rate of 60 s^{-1} [17,18].

Compared with other polymer dispersants, branched polyethylenimine (PEI) has a chemical structure [23], as shown in Fig. 1, which may exhibit better steric stabilization behavior. Besides, it has a high positive charge density that allows it to adsorb tightly on negatively charged substrates, resulting in a higher electrostatic force in a suspension. Therefore, as a strongly cationic branched polymer, PEI has been applied to disperse many kinds of ceramic suspensions [19–22].

In this present work, PEI was used as dispersant. The purpose of this work is to optimize and prepare a ZrB_2–SiC aqueous suspension with a high solid loading

---

*Corresponding author. Tel./fax: +86 451 86403016.
E-mail address: herujie2003jci@163.com (R. He).

0272-8842/$ - see front matter
http://dx.doi.org/10.1016/j.ceramint.2012.08.073

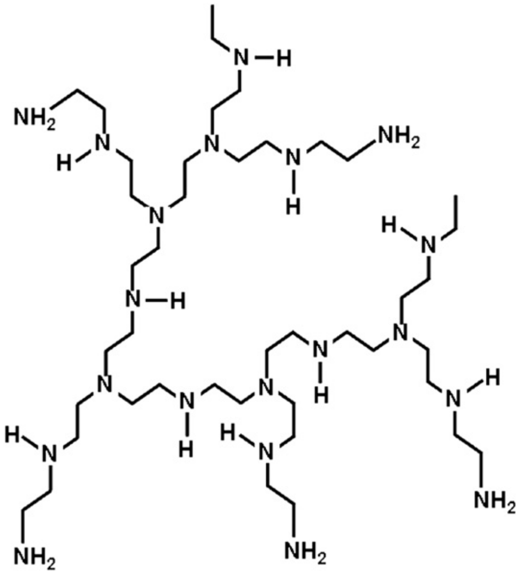

Fig. 1. Schematic drawing of the chemical structure of branched PEI.

and low viscosity. The effects of PEI concentration, pH value on dispersion of ZrB_2 and SiC in water, and rheological behavior of ZrB_2–SiC aqueous suspensions were investigated in detail. And the interparticle interactions in suspensions were calculated using a freeware, Hamaker 2 program [24]. Finally, a high solid loading, low viscosity ZrB_2–SiC aqueous suspension was successfully obtained.

2. Experimental procedure

2.1. Materials

Commercially available ZrB_2 powders (Northwest Institute for Non-ferrous Metal Research, Xi′an, China) and SiC powders (Weifang Kaihua Micro-powder Co. Ltd., Weifang, China) were used as raw materials. The ZrB_2 and SiC powders had the same purity of 99%. The median volume diameter (Dv50) for the as-purchased ZrB_2 and SiC powder was about 2 μm and 1 μm, respectively, reported by manufacturers. Polyethylene imine (PEI, Aladdin Co. Ltd., Shanghai, China), a cationic polymer with an average molecular weight of 10,000 was used as dispersant.

2.2. Suspension preparation

Firstly, the dispersion of ZrB_2 and SiC powders in water was investigated by zeta potential measurements and particle size distribution measurements. Then, ZrB_2–SiC composite suspensions were prepared by adding 80 vol% ZrB_2 plus 20 vol% SiC powder mixtures to deionized water. A series of ZrB_2–20SiC aqueous suspensions with different solid loading containing 0–0.8 wt% PEI dispersant (based on the powder mixture weight) were ball-milled for 20 h using ZrO_2 spherical grinding media in a planetary mill (MCA-10B, Nanjing University Instrument Plant, Nanjing, China) at 240 rpm (revolutions per minute). The pH values of the suspensions were adjusted using hydrochloric acid (HCl) and ammonia water (NH_4OH).

2.3. Measurements

Zeta potential measurements of ZrB_2 and SiC in the absence and presence of PEI were conducted separately as a function of pH value (in the range of 2–13) via Zeta potential analyzer (Zetasizer Nano ZS, Malvern, UK) using very dilute suspensions (0.01 vol%). The ionic strength was adjusted with 0.001 M KCl solutions. Particle size distributions of ZrB_2 and SiC powders in water (pH = 6–7) in the absence and presence of PEI were determined using a laser particle size analyzer (Hylology Instruments Co. Ltd., Dandong, China). Rheological behavior of the suspensions was determined using a rotational viscometer (4ARES-9a, Rheometric Scientific Inc., USA).

3. Interparticle interactions theory [24]

The interparticle interactions are predicted within the Derjaguin–Landau–Verwey–Overbeck (DLVO) model. The total interparticle interaction V is described as follows:

$$V = V_{VdW} + V_{electrostat} + V_{steric} \tag{1}$$

where V_{VdW}, $V_{electrostat}$ and V_{steric} are the attractive Van der Waals, the electrostatic and steric interactions, respectively. These interactions will briefly be outlined in the following.

3.1. Van der Waals forces

In a ceramic suspension system, V_{VdW} is calculated by Hamaker model as:

$$V_{VdW} = (A/6)\left[\frac{2a_1a_2}{d^2+2a_1d+2a_2d} + \frac{2a_1a_2}{d^2+2a_1d+2a_2d+4a_1a_2} + \ln\left(\frac{d^2+2a_1d+2a_2d}{d^2+2a_1d+2a_2d+4a_1a_2}\right)\right] \tag{2}$$

where A is the effective Hamaker constant for the system, d is the particle surface–surface separation and a_1 and a_2 are the ceramic particle radii, respectively. If in a mono-particle suspension system, there is only one kind of ceramic particle, thus $a_1 = a_2$.

3.2. Electrostatic interactions

Commonly, the electrostatic interaction, $V_{electrostat}$ is usually considered based on the Hogg–Healy–Füstenau (*HHF*) model. In this model, the dispersion medium is characterized by the ionic strength I_c as given by Eq. (3).

$$I_c = \frac{1}{2}\sum c_i z_i^2 \tag{3}$$

where c_i is the molar concentration of the ionic species i, having a valence z_i. The double layer formed at the particle surface is characterized by the Debye length (double layer thickness) κ^{-1} as given by Eq. (4).

$$\kappa^{-1} = \sqrt{\frac{\varepsilon_m \varepsilon_e kT}{2e^2} I_c 1000 N_A} \tag{4}$$

In this equation, ε_m and ε_e are the dielectric constant of the medium and the electric constant, respectively, k is Boltzmann's constant, T is the absolute temperature, e is the elementary charge and N_A is Avogadro's constant.

The surface potential Ψ is calculated from the measured zeta potential ζ via:

$$\psi = \xi \exp(\kappa d_s) \tag{5}$$

where d_s is the distance from the surface where the zeta potential is measured.

According to *HHF* model, the electrostatic interaction, $V_{electrostat}$ is calculated as follows,

$$V_{electrostat} = \frac{\pi \varepsilon_m \varepsilon_e a_1 a_2}{2a} \left[(\psi_1 + \psi_2)^2 \ln(1 + \exp(-\kappa h)) + (\psi_1 - \psi_2)^2 \ln(1 - \exp(-\kappa h)) \right] \tag{6}$$

3.3. Steric interactions

The hard-wall model introduced by Bergstrom works well for the steric interaction calculations. The interaction potential for this model is divided into three domains, h is the interparticle distance, the first being a fully interpenetrated domain at separations closer than the adsorbed layer thickness d_a, where the interaction potential is infinitely repulsive. The interpenetrated domain up to a separation of twice the adsorbed layer thickness is characterized by the molecule-solvent interaction χ, the molecular volume of the solvent V_s as well as the volume fraction of molecules in the adsorbed layer φ. At large separations the adsorbed molecules do not interact and the potential is consequently zero.

$$V_{steric} = \begin{cases} h < d_a : \infty \approx 10^6 \\ d_a \le h \le 2d_a : & \dfrac{2a_2}{a_1 + a_2} \left[\dfrac{\pi a_1 \kappa T}{V \varphi^2} \left(\dfrac{1}{2} - \chi \right) (2d_a - h)^2 \right] \\ h > 2\mathrm{d}_a : 0 \end{cases} \tag{7}$$

Based on these models, Bowen and his co-workers [24] developed a program, Hamaker 2 (download at http://hamaker.epfl.ch), to rapidly predict the particle interactions in ceramic powder suspensions and to gain important understanding of the delicate balance of forces in suspensions. Using this program, the interaction potentials can be calculated considering Van der Waals, electrostatic interaction and steric interaction in the ceramic suspensions. In their previous work, the Hamaker 2 toolkit was successfully demonstrated its usefulness in some detailed case studies. In this paper, the freeware, Hamaker 2, was therefore applied to calculate the interparticle potentials in the ceramic suspension and to predict the suspension stability.

4. Results and discussion

4.1. Dispersion of ZrB_2 and SiC in water

The stability of aqueous colloidal systems can be controlled by generating like-charge of sufficient magnitude on the surfaces of suspended ceramic particles. The resulting repulsive potential energy, $V_{electrostat}$, exhibits exponential distance dependence. Its strength depends on the surface potential induced on the interacting colloidal particles and the dielectric properties of the intervening medium. The electrostatic potential for ceramic particles, for example ZrB_2, follows the well known interacting double layer model. Zeta potential is usually used as a criterion for surface charge because it is close to the Stern potential and it can be measured. Zeta potential is a shear plan potential. Generally, the zeta potential reflects the electrostatic dispersion effect. The higher the relative zeta potential (measured in mV), the better the dispersion of the powder in the medium. Besides, steric stabilization also provides a route to control the suspension stability. When two ceramic particles with adsorbed polymer layers approach each other at a distance of less than twice the thickness of the adsorbed layer, interaction occurs between the two layers.

Fig. 2 (a and b) show the zeta potential curves of ZrB_2 and SiC powder in deionized water in the absence and presence of PEI, respectively. The isoelectric point (IEP, the pH which the net charge on the particle surface is zero) for pristine ZrB_2 and SiC powder was ~6.7 and ~4.2, respectively. With the increasing of pH, a steep increase of the zeta potential was observed. The absolute value of zeta potentials for both ZrB_2 and SiC reached the maximum at pH value of about 11. And the absolute maximum zeta potential for pristine ZrB_2 and SiC was about 43 and 48 mV, respectively. When PEI was added, the IEPs for both ZrB_2 and SiC were displaced towards higher pHs. The absolute maximum zeta potential for both ZrB_2 and SiC suspension was obtained when using 0.6 wt% PEI as dispersant at pH value of 6–7. The maximum zeta potential for ZrB_2 and SiC suspension were about 63 and 72 mV, respectively. Compared with the zeta potential of ZrB_2 and SiC without dispersant, the absolute value of maximum increased by about 20 and 24 mV, respectively.

On one hand, when PEI concentration below 0.6 wt%, a lower relative zeta potential was probably due to a lower particle surface coverage, inducing lower electrostatic repulsion between particles thereby leading to an insufficient repulsive barrier to avoid the formation of agglomerates. On the other hand, when PEI concentration above 0.6 wt%, the relative low zeta potential resulted from the over-saturated adsorption of PEI onto particle surface, which not only increased the ionic strength of the solution and compressed the double layer, resulting in the electrostatic repulsion decrease between particles, but also increased the bridging flocculation because of polyelectrolyte macromolecule. Both of unsaturated adsorption and

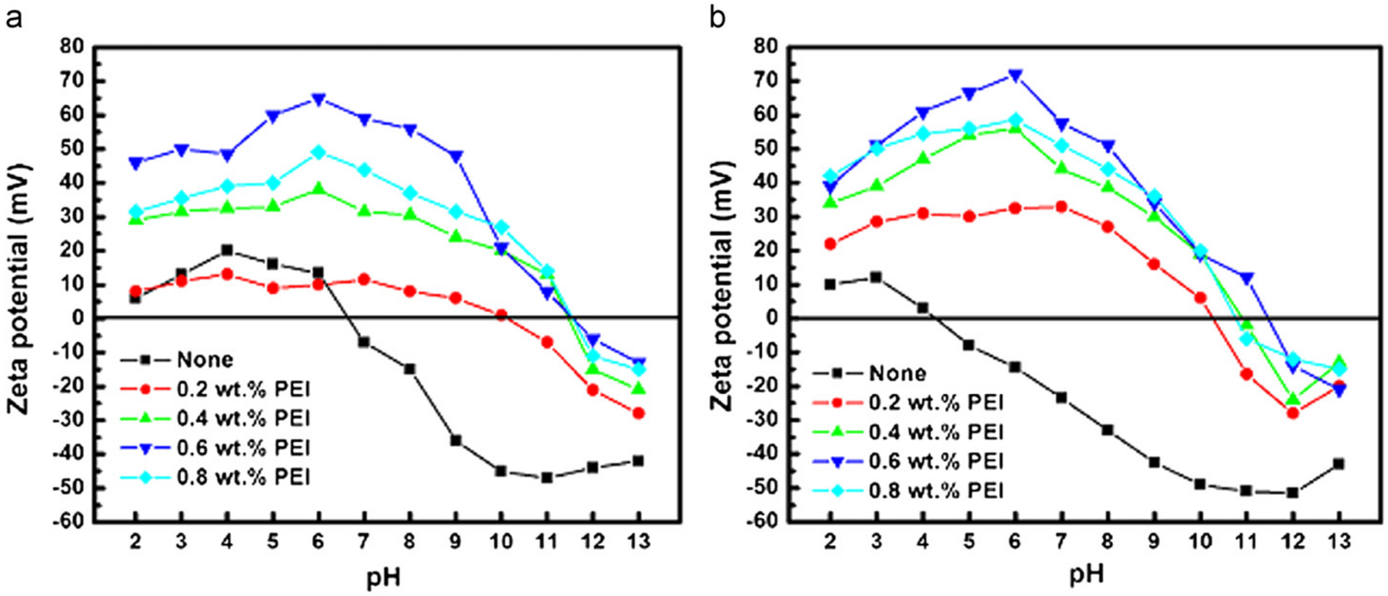

Fig. 2. Zeta potentials of a) ZrB_2 and b) SiC in the absence and presence of PEI.

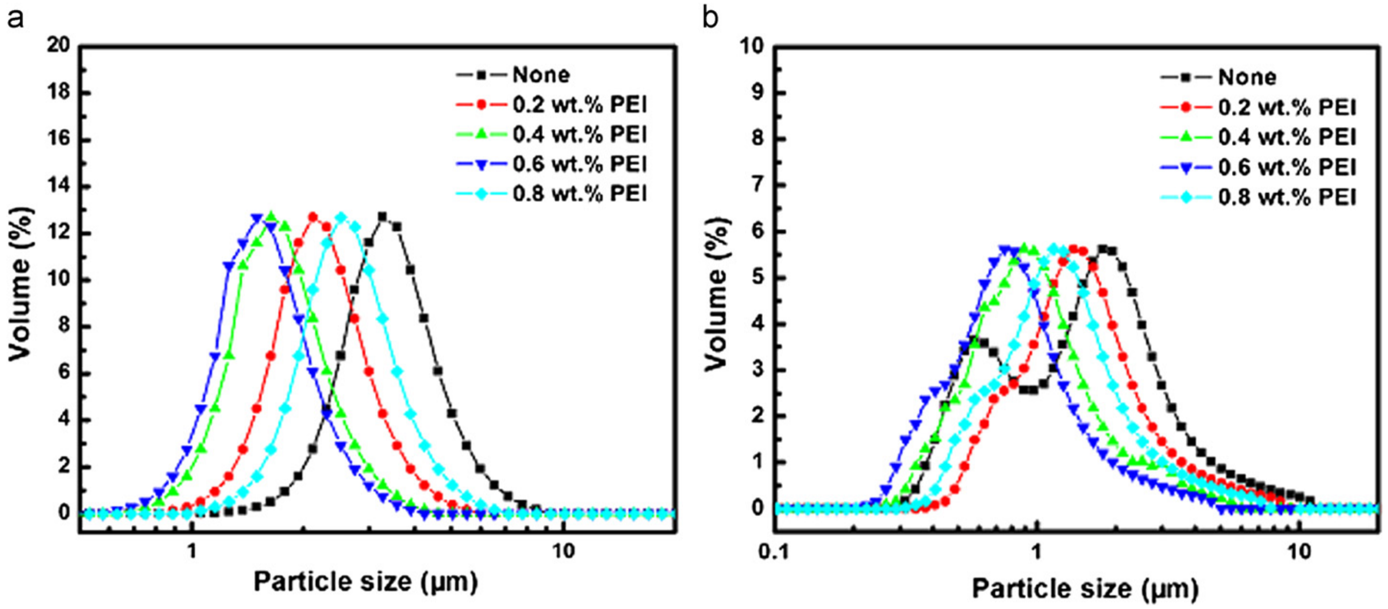

Fig. 3. Particle size distributions of a) ZrB_2 and b) SiC in the absence and presence of PEI.

over-saturated adsorption were harmful to the particle dispersing. Therefore, both ZrB_2 suspension and SiC suspension can achieve a well-dispersed state using 0.6 wt% PEI as dispersant at pH 6–7. Detailed interparticle interactions will be calculated in Section 4.2.

Fig. 3 (a and b) give the particle size distributions of ZrB_2 and SiC powder in the absence and presence of PEI, respectively. The particle size distribution of a powder is a key characteristic that influences its properties [25]. The measured median volume diameter (Dv50) for pristine ZrB_2 and SiC powder was 2.10 μm and 1.47 μm, respectively, which were slightly higher than the data given by the suppliers. The Dv50 for pristine ZrB_2 and SiC powder without dispersant and with different concentrations of PEI, were clearly listed in Table 1. When doped with PEI, the median volume diameter (Dv50) for both ZrB_2 and SiC were much smaller than those of un-doped powders. When adding 0.6 wt% PEI, both ZrB_2 and SiC had the smallest Dv50 for the reason that both of unsaturated adsorption and over-saturated adsorption were harmful to the particle dispersing. The median volume diameter (Dv50) of ZrB_2 and SiC with 0.6 wt%

PEI were about 1.72 μm and 0.60 μm, respectively. Therefore, the optimum dispersant concentration for both ZrB_2 and SiC ceramic powders should be around 0.6 wt%.

4.2. Interparticle potential calculation

In our study, a freeware (Hamaker 2 program developed by Paul Bowen and his co-workers) was used to calculate the interparticle interactions between particles and to assess the stability of the ZrB_2 and SiC suspensions, respectively. Table 1 lists the data used for interparticle potential calculations through Hamaker 2 toolkit.

For interparticle interactions, Hamaker constant A can be calculated by the following equation [26]:

$$A=(3/4)kT\left(\frac{\varepsilon_p-\varepsilon_m}{\varepsilon_p+\varepsilon_m}\right)^2+\frac{3h\omega({n_p}^2-{n_m}^2)^2}{16\sqrt{2}({n_p}^2+{n_m}^2)^{3/2}} \tag{8}$$

where h is Planck's constant, $h=6.626\times10^{-34}$ J s, k is Boltzmann's constant, $k=1.381\times10^{-23}$ J/K, T is the absolute temperature, $T=300$ K. n_p and n_m are the index of refraction of particles and medium, respectively. ε_p and ε_m are the dielectric constants of particles and medium, respectively. ω is UV adsorptive frequency, $\omega=3.0\times10^{15}\,s^{-1}$. Since the medium is water in this study, $\varepsilon_m=78.36$ F/m and $n_m=1.3$. The dielectric constants of ZrB_2 and SiC are supposed to be 10. The index of refraction of ZrB_2 and SiC are 1.77 and 2.65, respectively. Consequently, Hamaker constant A of ZrB_2 and SiC calculated by Eq. (8) is 1.16×10^{-19} and 8.42×10^{-19} J, respectively.

Fig. 4 shows the interparticle potential calculation results for ZrB_2 and SiC in the absence and presence of PEI using Hamaker 2 program. It was found that the ZrB_2 suspensions without dispersant and with 0.2 wt% PEI had attractive interparticle potentials, which meant the ZrB_2 particles would attract and aggregate, leading to agglomeration and instability

Table 1
The data used for interparticle interactions calculations.

Powder	pH value	Zeta potential (mV)	Zeta plane (nm)[a]	Ionic strength (M)	Particle density (g/cm^3)	Particle diameter (Dv50) (μm)	Hamaker constant ($\times10^{-19}$ J)
ZrB_2	6	13.5	5	0.001	6.09	2.10	1.16
ZrB_2—0.2 wt% PEI	6	10	4	0.001	6.09	1.88	1.16
ZrB_2—0.4 wt% PEI	6	38	2	0.001	6.09	1.75	1.16
ZrB_2—0.6 wt% PEI	6	65	1	0.001	6.09	1.72	1.16
ZrB_2—0.8 wt% PEI	6	49	0.5	0.001	6.09	2.00	1.16
SiC	6	−14.5	5	0.001	3.21	1.47	8.42
SiC—0.2 wt% PEI	6	32.5	4	0.001	3.21	1.25	8.42
SiC—0.4 wt% PEI	6	56	2	0.001	3.21	1.03	8.42
SiC—0.6 wt% PEI	6	72	1	0.001	3.21	0.60	8.42
SiC—0.8 wt% PEI	6	58.5	0.5	0.001	3.21	0.92	8.42

[a] When PEI unsaturated adsorbed on the particle surface, the zeta plane thickness became high. When PEI over-saturated adsorbed on the particle surface, the double layer and zeta plane layer became compressed. Therefore, the thickness of the zeta plane with 0, 0.2, 0.4, 0.6 and 0.8 wt% PEI for both ZrB_2 and SiC particle are assumed to be 5, 4, 2, 1 and 0.5 nm, respectively.

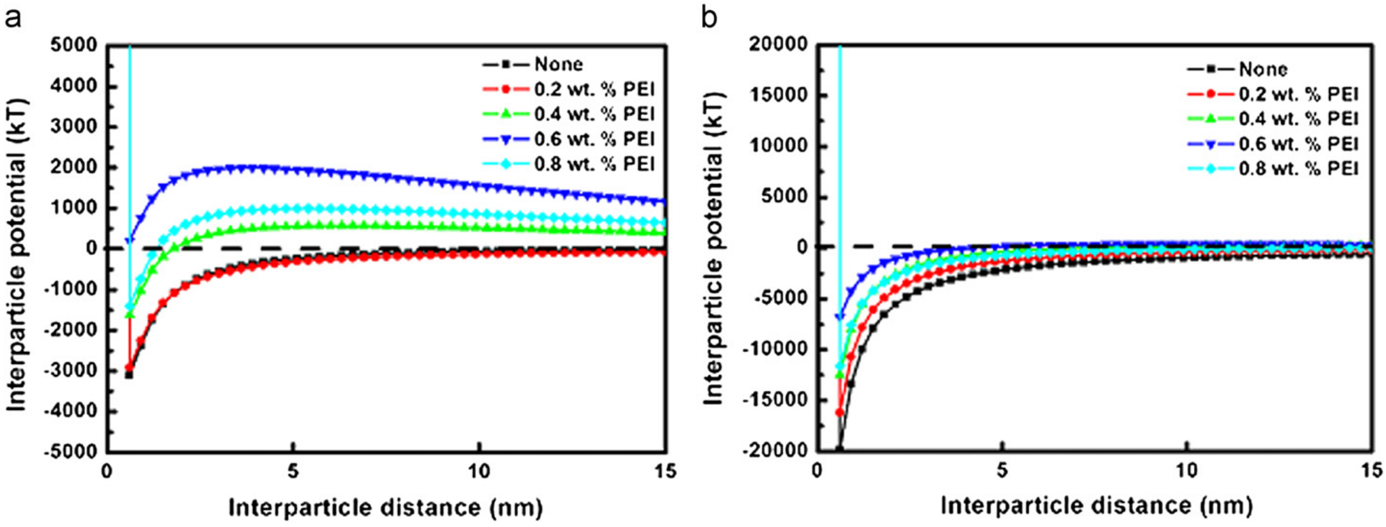

Fig. 4. Interparticle potential calculations for a) ZrB_2 and b) SiC.

of these ceramic suspensions. The ZrB_2 suspensions with 0.4 and 0.8 wt% PEI were attractive in the interparticle distance of 0–2 nm, and repulsive above 2 nm. However, the interparticle potential for suspension with 0.6 wt% PEI was repulsive, indicating the ZrB_2 particles would repulse each other and finally formed a stable suspension. For SiC suspensions, all potentials are attractive, meaning that SiC particles could strongly attract each other. However, SiC suspension with 0.6 wt% had the lowest attractive interparticle interaction, indicating that this suspension was the most well-dispersed. These interparticle potential calculation results agreed very well with the experimental results. Consequently, 0.6 wt% PEI was the optimum dispersant concentration for both ZrB_2 and SiC suspension.

4.3. *Rheological behavior of ZrB_2–SiC suspensions*

As for ZrB_2–SiC composite suspensions, the influence of pH values on rheological properties is very important and a suitable pH value is helpful for enhancing the solid loading as well as reducing the viscosity of the suspension. To identify the optimum pH value for stable suspensions, the pH value was adjusted to review the variety of viscosities of the ZrB_2–SiC aqueous suspensions, as shown in Fig. 5. The lowest viscosity was obtained at the pH value of 6. This agreed with the results of zeta potential measurements and particle size distribution measurements, indicating the optimum pH value of ZrB_2–SiC aqueous suspension was 6.

As discussed above, the changes in zeta potentials of ZrB_2 and SiC particles indicated strong differences interparticle forces, from adhesive at the IEPs to strongly repulsive at lower and higher pH values, respectively. Thus, the changes in zeta potentials would affect the rheological behavior of ZrB_2–SiC aqueous suspensions. Fig. 6 exhibits the viscosities of ZrB_2–SiC aqueous suspension as a function of shear rate with different concentrations of PEI. The rheological properties of the ZrB_2–SiC aqueous suspensions were strongly dependent on the amounts of PEI added. The suspension with 0.6 wt% PEI had the lowest viscosity. Using 0.6 wt% PEI as dispersant seemed to be the optimum dispersant concentration to disperse the ZrB_2–SiC powder mixture, which also induced the minimum viscosity value (as shown in Fig. 6) and the maximum zeta potentials.

According to above results and discussion, in our study, ZrB_2–SiC aqueous suspensions with different solid loadings were prepared using 0.6 wt% PEI as dispersant at pH 6. The viscosities of the suspensions as a function of solid loading are given in Fig. 7. A well-stabilized ZrB_2–SiC aqueous suspension with a high solid loading (up to 52 vol%) and low viscosity (980 mPa · s at 100 s^{-1}) was successfully prepared.

It is well known that solid loading directly relates to the green density of the ceramic. High solid loading can inhibit

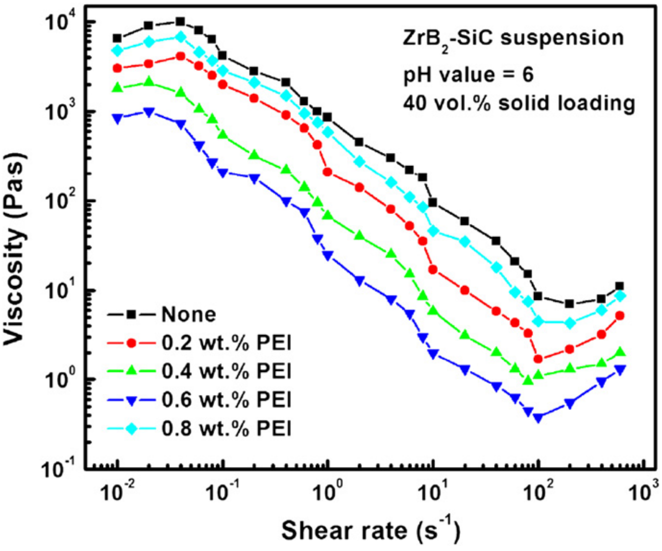

Fig. 6. Viscosity of ZrB_2–SiC aqueous suspension vs. PEI concentration.

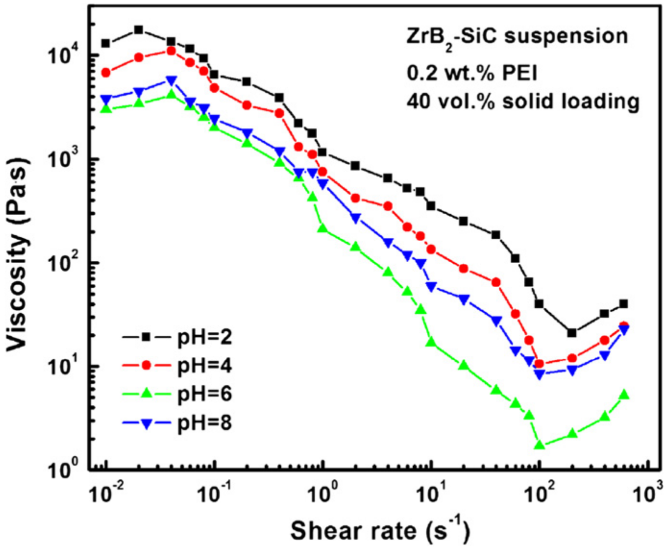

Fig. 5. Viscosity of ZrB_2–SiC aqueous suspension vs. pH value.

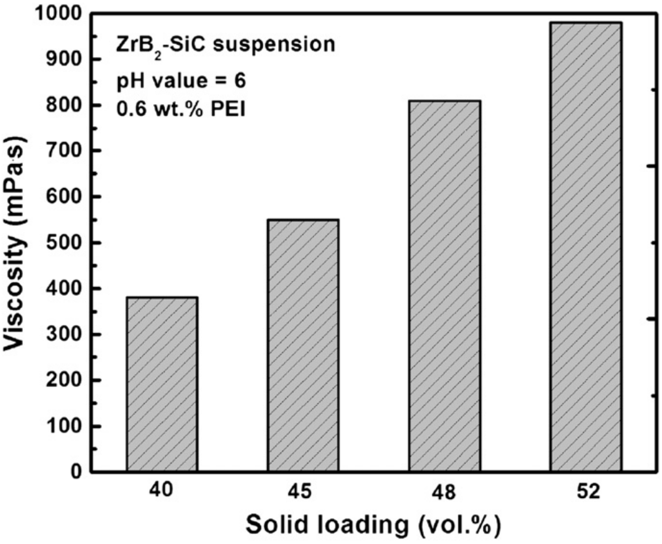

Fig. 7. Viscosity of ZrB_2–SiC aqueous suspension (100 s^{-1}) vs. solid loading.

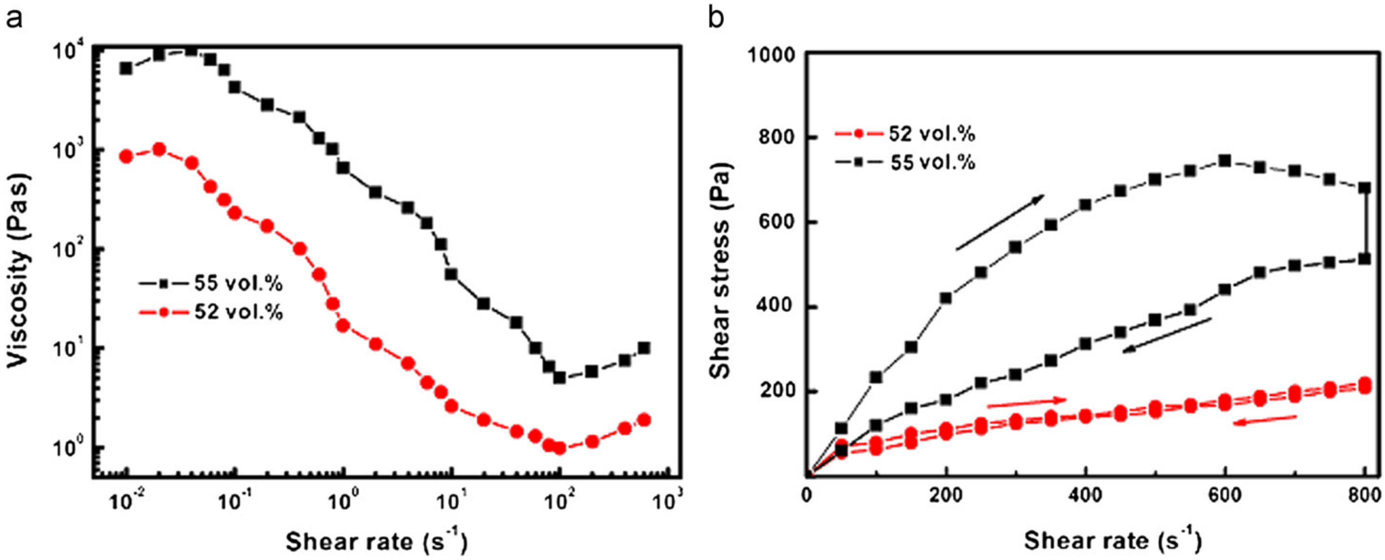

Fig. 8. Rheological behavior of 52 vol% and 55 vol% suspensions: (a) viscosity and (b)shear stress.

defect formation during the colloidal forming process and the following drying stage. The rheological behavior of 52 and 55 vol% ZrB_2–SiC suspensions (in the presence of 0.6 wt% PEI at pH 6) was presented in Fig. 8. At the shear rate of 100 s−1, the viscosity for 52 and 55 vol% solid loading suspensions was 980 mPa · s and ~5 Pa · s, respectively. The viscosity of 55 vol% suspension was higher (at a shear rate of 100 s^{-1}) and exhibited a more obvious "shear thickening" behavior [27]. The shear thickening behavior was undesirable for the following colloidal forming process. It is well known that ceramic particles tend to move rapidly and attract each other at high shear rates, yet the suspension got an increased viscosity of the suspension at high solid loading. However, the viscosity of 52 vol% suspension was significantly lower than the 55 vol% suspension. The 52 vol% suspension exhibited a slighter "shear thickening" behavior. In the suspension, the ceramic particles formed aggregated structure firstly, yet the shear rate increased, the shear stress increased correspondingly. Then the aggregated structure broke up and some of the ceramic particles were free to move quickly. In addition, the suspensions exhibited some time dependency behavior.

5. Conclusions

In this paper, PEI was selected as the dispersant for the aqueous dispersion of ZrB_2, SiC and ZrB_2–20SiC powder mixture. The effects of the dispersant concentrations and pH values on zeta potentials and particle size distribution of ZrB_2 and SiC powders were investigated in detail. Well-dispersed ZrB_2 suspension and SiC suspension were obtained by using 0.6 wt% PEI at pH 6. The interparticle interactions in ZrB_2 and SiC suspensions were calculated using a freeware, Hamaker 2 program. The calculated results agreed very well with the experimental results. The rheological behavior of ZrB_2–SiC aqueous suspensions was also studied and discussed. It was found that the 52 vol% suspension had a lower viscosity and exhibited a slighter "shear thickening" behavior, whereas the 55 vol% suspension had a much higher viscosity and exhibited a more obvious "shear thickening" behavior. Considering high solid loading and low viscosity are desirable for the following colloidal forming processes, a high solid loading (up to 52 vol%), low viscosity (980 mPa s at 100 s^{-1}) ZrB_2–SiC aqueous suspension was successfully prepared by using 0.6 wt% PEI at pH 6 and ball milled at 240 rpm for 20 h. We believe that this study will be helpful for the preparation of high quality ZrB_2–SiC suspension and lay the foundation for aqueous colloidal forming of ZrB_2–SiC composites.

Acknowledgements

This research was financially supported by the National Science Foundation of China (No. 510702042 and 50972029) and the Fundamental Research Funds for Central Universities (HIT. NSRIF. 2012030). The authors wish to express sincere thanks to Prof. Paul Bowen and his co-workers in Laboratoire de Technologie des Poudres, Ecole Polytechnique Fédérale de Lausanne (EPFL), Switzerland for their kind efforts in the development of Hamaker 2 freeware and their previous work in suspension stability calculations and predictions. The authors also thank the editors and reviewers for the discussion and revision of the manuscript.

References

[1] P. Hu, Z. Wang, Flexural strength and fracture behavior of ZrB_2–SiC ultra-high temperature ceramic composites at 1800 °C, Journal of the European Ceramic Society 30 (2010) 1021–1026.

[2] J.W. Zimmermann, G.E. Hilmas, W.G. Fahrenholtz, Thermal shock resistance of ZrB_2 and ZrB_2–30% SiC, Materials Chemistry and Physics 112 (2008) 140–145.

[3] P. Hu, G.L. Wang, Z. Wang, Oxidation mechanism and resistance of ZrB_2–SiC composites, Corrosion Science 51 (2009) 2724–2732.

[4] S.Q. Guo, T. Mizuguchi, M. Ikegami, Y. Kagawa, Oxidation behavior of ZrB_2–$MoSi_2$–SiC composites in air at 1500 °C, Ceramics International 37 (2011) 585–591.

[5] S.Q. Guo, Y. Kagawa, T. Nishimura, H. Tanaka, Elastic properties of spark plasma sintered (SPSed) ZrB_2–ZrC–SiC composites, Ceramics International 34 (2008) 1811–1817.

[6] F. Monteverde, R. Savino, Stability of ultra-high-temperature ZrB_2–SiC ceramics under simulated atmospheric re-entry conditions, Journal of the European Ceramic Society 27 (2007) 4797–4805.

[7] S.R. Levine, E.J. Opila, M.C. Halbig, J.D. Kiser, M. Singh, J.A. Salem, Evaluation of ultra-high temperature ceramics for aeropropulsion use, Journal of the European Ceramic Society 22 (2002) 2757–2767.

[8] X.H. Zhang, P. Hu, J.C. Han, S.H. Meng, Ablation behavior of ZrB_2–SiC ultra high temperature ceramics under simulated atmospheric re-entry conditions, Composites Science and Technology 68 (2008) 1718–1726.

[9] W.G. Fahrenholtz, G.E. Hilmas, I.G. Talmy, J.A. Zaykoski, Refractory diborides of zirconium and hafnium, Journal of the American Ceramic Society 90 (2007) 1347–1364.

[10] V. Medri, C. Capiani, A. Bellosi, Properties of slip-cast and pressureless-sintered ZrB_2–SiC composites, International Journal of Applied Ceramic Technology 8 (2011) 351–359.

[11] V. Medri, C. Capiani, D. Gardini, Slip casting of ZrB_2–SiC composite aqueous suspensions, Advanced Engineering Materials 12 (2010) 210–215.

[12] Z.H. Lü, D.L. Jiang, J.X. Zhang, Q.L. Lin, Aqueous tape casting of zirconium diboride, Journal of the American Ceramic Society 92 (2009) 2212–2217.

[13] Z.H. Lü, D.L. Jiang, J.X. Zhang, Q.L. Lin, Microstructure and mechanical properties of zirconium diboride obtained by aqueous tape casting process and hot pressing, Journal of the American Ceramic Society 93 (2010) 4153–4157.

[14] Z.H. Lü, D.L. Jiang, J.X. Zhang, Q.L. Lin, Processing and properties of ZrB_2–SiC composites obtained by aqueous tape casting and hot pressing, Ceramics International 37 (2011) 293–301.

[15] S.L. Natividad, V.R. Marotto, L.S. Walker, D. Pham, Tape casting thin, continuous, homogenous, and flexible tapes of ZrB2, Journal of the American Ceramic Society 94 (2011) 2749–2753.

[16] T.S. Huang, G.E. Hilmas, W.G. Fahrenholtz, M.C. Leu, Dispersion of zirconium diboride in an aqueous high-solids paste, International Journal of Applied Ceramic Technology 4 (2007) 470–479.

[17] R.J. He, X.H. Zhang, P. Hu, C. Liu, W.B. Han, Aqueous gelcasting of ZrB_2–SiC ultra high temperature ceramics, Ceramics International 38 (2012) 5411–5418.

[18] R.J. He, P. Hu, X.H. Zhang, C. Liu, Gelcasting of complex-shaped ZrB_2–SiC ultra high temperature ceramic components, Materials Science and Engineering A 556 (2012) 494–499.

[19] S.H. Lee, Y. Sakka, Y. Kagawa, Dispersion behavior of ZrB_2 powder in aqueous solution, Journal of the American Ceramic Society 90 (2007) 3455–3459.

[20] J. Sun, L. Gao, Dispersion SiC powder and improving its rheological behaviour, Journal of the European Ceramic Society 21 (2001) 2447–2451.

[21] J.X. Zhang, M. Iwasa, D.L. Jiang, Dispersion of SiC in aqueous media with Al_2O_3 and Y_2O_3 as sintering additives, Journal of the American Ceramic Society 88 (2005) 1013–1016.

[22] J.X. Zhang, F. Ye, D.L. Jiang, M. Iwasa, Dispersion of Si_3N_4 powders in aqueous media, Colloids and Surfaces, A: Physicochemical and Engineering Aspects 259 (2005) 117–123.

[23] B.C. Ong, Y.K. Leong, S.B. Chen, Interparticle forces in spherical monodispersed silica dispersions: effects of branched polyethylenimine and molecular weight, Journal of Colloid and Interface Science 337 (2009) 24–31.

[24] U. Aschauer, O. Burgos-Montes, R. Moreno, P. Bowen, Hamaker 2: a toolkit for the calculation of particle interactions and suspension stability and its application to mullite synthesis by colloidal methods, Journal of Dispersion Science and Technology 32 (2011) 470–479.

[25] P. Bowen, Particle size distribution measurement from millimeters to nanometers and from rods to platelets, Journal of Dispersion Science and Technology 23 (2002) 631–662.

[26] T. Zhou, H.Z. Li, Estimation of agglomerate size for cohesive particles during fluidization, Powder Technology 101 (1999) 57–62.

[27] R.J. Flatt, P. Bowen, Yodel: a yield stress model for suspensions, Journal of the American Ceramic Society 89 (2006) 1244–1256.